Non-oscillatory Central Schemes for Hyperbolic Conservation Laws

Doron Levy*

Introduction

In recent years, there was an enormous amount of successful activity in the construction, analysis and implementation of modern numerical algorithms for the approximate solution of nonlinear hyperbolic conservation laws. A large variety of accurate, high-resolution methods were developed and investigated, e.g. [8], [20], [37] and the references therein. Godunov-type schemes are a primary example for these modern high-resolution schemes. Such schemes are based on piecewise-polynomial reconstruction of point-values from cell averages, followed by the evolution of approximate fluxes. We distinguish between *upwind* and *central* Godunov-type schemes. The difference between these two types, lies in the way they realize the evolution of these piecewise-polynomials: upwind schemes sample the reconstructed values at the mid-cells. They necessitate characteristic information (approximate Riemann solvers...) and dimensional splitting, consult [9],[19] and [30], for example. Central schemes are based on *staggered* sampling at the interfacing breakpoints. Their main advantage is simplicity, consult [7],[29] and [14].

To be more specific, we concentrate on high-order multidimensional extensions of the non-oscillatory, second-order central Nessyahu-Tadmor (NT) scheme [29] (see also [34]). The central framework starts, at each time-level, with a non-oscillatory piecewise-linear approximation which is reconstructed from the piecewise-constant numerical data. This piecewise-linear approximation is evolved to the next time level and then realized by its piecewise-constant projection. The projection is based on *staggered* averaging which covers both left going and right going waves centered at each mid-cell. Consequently, the evolution step utilizes *smooth* numerical fluxes, which are bounded away from the center of the discontinuous Riemann fans. Here, approximate quadrature rules can replace the costly (approximate) Riemann solvers embedded in upwind schemes. It is therefore natural to use this central framework in more than one space dimension – where we avoid Riemann solvers and dimensional splitting.

We note that the *central* schemes were successfully implemented for a variety of problems, such as, e.g., the incompressible Euler equations [25], [18],[16],[17], the magneto-hydrodynamics equations [38], hyperbolic systems with relaxation source terms [4], [1],[31], non-linear optics [6], [32] and slow moving shocks [15].

---

*Département de Mathématiques et d'Informatique, Ecole Normale Supérieure, 45 rue d'Ulm, 75230 Paris Cedex 05, France; Email: dlevy@dmi.ens.fr

This paper is organized as follows. We begin in §1 by constructing the one-dimensional, non-oscillatory central schemes. Utilizing a high-order reconstruction, we extend the familiar first-order Lax-Friedrichs (LxF) scheme to high-orders: the second-order Nessyahu-Tadmor (NT) scheme presented in [29], and the third-order scheme [28] (see also [11],[5],[22]). We then proceed in §2 to the two-dimensional framework, focusing on the second-order, non-oscillatory central scheme [14] (see also [3],[2]). For a third-order scheme for 2D incompressible flows we refer to [21] and in the context of compressible flows to [23]. A general mechanism which transformed staggered schemes into non-staggered schemes without loss of accuracy was presented in [12].

1 Non-Oscillatory Central Schemes - The One-Dimensional Framework

1.1 The First-Order Lax-Friedrichs (LxF) Scheme

We approximate solutions to the one-dimensional hyperbolic system of conservation laws

$$u_t + f(u)_x = 0, \tag{1.1}$$

subject to the prescribed initial data, $u(x,t=0) = u_0(x)$. For simplicity, we assume an equally spaced grid, $\Delta x = x_{j+1} - x_j$, and by $\bar{w}_j^n$ we abbreviate the approximate cell-average at time $t = t^n$, associated with the cell $I_j := \{|x - x_j| \leq \frac{1}{2}\}$. We also denote by $\chi_j(x)$, the characteristic function of the cell I_j, i.e., $\chi_j(x) := 1_{I_j}$.

The staggered LxF approximation to (1.1) can be, e.g., derived by constructing a piecewise-constant interpolant through the given cell-averages, $w(x,t^n) = \sum_j \bar{w}_j^n \chi_j(x)$. This interpolant is then evolved exactly in time according to the conservation law (1.1), and finally projected onto its staggered cell-averages at the next time level.
For $\Delta t \max_u |f'(u)| \leq \frac{\Delta x}{2}$, the exact solution of (1.1) remains smooth at the integer grid points, x_{j-1}, x_j. Consequently, the required integrals of the fluxes are evaluated in terms of their constant initial data, without using any (approximate) Riemann solvers. The difference between the staggered cell-averages, $\bar{w}_{j+\frac{1}{2}}^{n+1} - \bar{w}_{j+\frac{1}{2}}^n$, equals to the difference between the averages of the fluxes over the staggered control-volume, and hence, the LxF scheme amounts to

$$\bar{w}_{j+\frac{1}{2}}^{n+1} = \frac{1}{2}(\bar{w}_j^n + \bar{w}_{j+1}^n) - \lambda \left[f(w_{j+1}^n) - f(w_j^n) \right]. \tag{1.2}$$

The LxF scheme (1.2) is very robust, but it suffers from excessive dissipation. To overcome this dissipation, while retaining the stability properties of the LxF scheme, we proceed with

1.2 The Second-Order Nessyahu-Tadmor (NT) Scheme

The NT scheme is based on reconstructing a piecewise-linear (MUSCL-type) interpolant from the known staggered cell-averages at time t^n (see figure 1.1),

$$w(x,t^n) = \sum_j p_j(x)\chi_j(x) := \sum_j \left[\bar{w}_j^n + w_j' \left(\frac{x - x_j}{\Delta x} \right) \right] \chi_j(x). \tag{1.3}$$

Here and below, w'_j, denote the discrete slopes which are reconstructed from the given cell-averages. A possible computation of these slopes which results in an overall non-oscillatory scheme (consult [29]), is given by the family of *discrete derivatives* parameterized with $1 \leq \theta \leq 2$:

$$w'_j = MM(\theta \Delta v_{j+1/2}, \frac{1}{2}(\Delta v_{j-1/2} + \Delta v_{j+1/2}), \theta \Delta v_{j-1/2}), \tag{1.4}$$

Here, Δ denotes the centered differencing $\Delta v_{j+1/2} = v_{j+1} - v_j$, and MM denotes the Min-Mod non-linear limiter

$$MM\{x_1, x_2, ...\} = \begin{cases} \min_j\{x_j\} & \text{if } x_j > 0, \forall j \\ \max_j\{x_j\} & \text{if } x_j < 0, \forall j \\ 0 & \text{otherwise.} \end{cases} \tag{1.5}$$

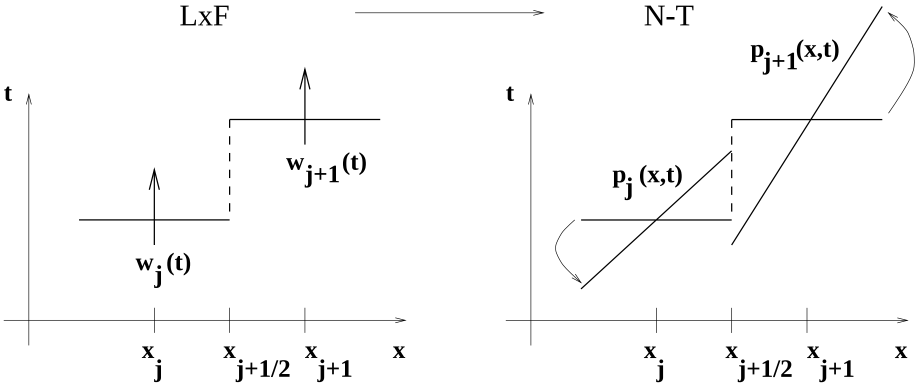

Figure 1.1: The second-order reconstruction

This interpolant (1.3) is then evolved exactly in time and projected on the staggered cell-averages on the next time-step, t^{n+1}, resulting with the two-step *predictor-corrector* form,

$$\begin{aligned} w_j^{n+\frac{1}{2}} &= w_j^n - \frac{\lambda}{2} f'_j, & (1.6) \\ \bar{w}_{j+\frac{1}{2}}^{n+1} &= \frac{1}{2}(\bar{w}_j^n + \bar{w}_{j+1}^n) + \frac{1}{8}(w'_j - w'_{j+1}) - \lambda \left[f(w_{j+1}^{n+1/2}) - f(w_j^{n+1/2}) \right]. & (1.7) \end{aligned}$$

The discrete derivatives of the flux f'_j can be computed, e.g., by $f'_j = A_j^n w'_j$, with $A_j^n := A(\bar{w}_j^n) = f_u(\bar{w}_j^n)$; alternatively, one can apply the MinMod limiter to each of the components of f. This component-wise approach is one of the main advantages offered by the central NT schemes over the corresponding characteristic decompositions required by upwind schemes – consult the discussion in [29], [14].

1.3 The Third-Order Liu-Tadmor Scheme

The staggered third-order central scheme presented by Liu and Tadmor in [28], is based on a non-oscillatory third-order reconstruction by Liu and Osher [26], $w(x, t^n) = \sum_j p_j(x) \chi_j(x)$. Here, each quadratic piece, $p_j(x)$, is of the form

$$p_j(x) = w_j^n + w'_j \left(\frac{x - x_j}{\Delta x} \right) + \frac{1}{2} w''_j \left(\frac{x - x_j}{\Delta x} \right)^2. \tag{1.8}$$

We seek for a reconstruction (1.8), that satisfies the following properties:

- **Conservation.** Conserving the given cell-averages

$$\bar{w}(x,t^n)|_{x=x_j} = \bar{w}^n_j. \tag{1.9}$$

- **Accuracy.** Third-order accuracy

$$w(x,t^n) = u(x,t^n) + O((\Delta x)^3). \tag{1.10}$$

- **Shape-preserving.** $p_j(x)$ has the same shape as $\sum_{i=j-1}^{j+1} \bar{w}^n_i \chi_i$.
- **Non-oscillatory.** The piecewise-quadratic reconstruction is non-oscillatory in the sense that

$$sgn(p_{j+1}(x_{j+\frac{1}{2}}) - p_j(x_{j+\frac{1}{2}})) = sgn(\bar{w}^n_{j+1} - \bar{w}^n_j). \tag{1.11}$$

Due to those requirements (1.9)-(1.11), the reconstructed discrete first and second derivatives are uniquely given by

$$w'_j := \theta_j \Delta_0 \bar{w}^n_j, \qquad w''_j := \theta_j \Delta_+ \Delta_- \bar{w}^n_j. \tag{1.12}$$

The parameter θ_j is a non-linear limiter designed to prevent oscillations (consult [26] and [28] for specific details on the construction of such a non-linear limiter). We used the usual notations for one-sided and centered differencing, $\Delta_\pm \bar{w}_j = \pm(\bar{w}_{j\pm 1} - \bar{w}_j)$ and $\Delta_0 = \frac{1}{2}(\Delta_+ - \Delta_-)$. Here, $w^n_j := \bar{w}^n_j - \frac{w''_j}{24}$, are the reconstructed point-values which starting with the third-order reconstruction are not necessarily equal to the cell-averages.

As in the first-order and second-order schemes, an exact evolution of this piecewise-quadratic reconstruction, followed by a projection on the staggered averages yields the scheme which can be formalized in terms of a *predictor* step

$$w^{n+\alpha}_j = w^n_j + \lambda\alpha \dot{w}^n_j + \frac{(\lambda\alpha)^2}{2}\ddot{w}^n_j, \qquad \alpha = \frac{1}{2}, 1, \tag{1.13}$$

followed by the *corrector*

$$\begin{aligned} \bar{w}^{n+1}_{j+\frac{1}{2}} = \frac{1}{2}(\bar{w}^n_j + \bar{w}^n_{j+1}) + \frac{1}{8}(w'_j - w'_{j+1}) - \frac{\lambda}{6}\Big\{ & [f(w^n_{j+1}) + 4f(w^{n+1/2}_{j+1}) + f(w^{n+1}_{j+1})] \\ & -[f(w^n_j) + 4f(w^{n+1/2}_j) + f(w^{n+1}_j)]\Big\}. \end{aligned} \tag{1.14}$$

The 'dotted' notation, $\dot{w}^n_j, \ddot{w}^n_j$, abbreviates the first and the second time-derivatives, respectively:

$$\begin{aligned} \dot{w}^n_j &= (\Delta x \cdot \partial_t) w(x_j,t^n) = -\Delta x \cdot \partial_x f(w(x_j,t^n)) = -a(w^n_j) \cdot w'_j, \\ \ddot{w}^n_j &= (\Delta x \cdot \partial_t)^2 w(x_j,t^n) = \Delta x \cdot \partial_x \left[a(w^n_j) \Delta x \cdot \partial_x f(w(x_j,t^n))\right] \\ &= a^2(w^n_j) w''_j + 2a(w^n_j) a'(w^n_j)(w'_j)^2. \end{aligned}$$

The construction of this scheme is based on a more accurate Taylor expansion to predict the mid-values, as well as on the Simpson's time-integration method which provides the required accuracy in time

$$\frac{1}{\Delta x}\int_{\tau=t^n}^{t^{n+1}} f(w(x_{j,\tau})) \sim \frac{\lambda}{6}\left[f(w_j^n)+4f(w_j^{n+1/2})+f(w_j^{n+1})\right].$$

We note that the choice of the limiter θ_j in [28], implies that $N(w(\cdot,t^n))$ – the number of extrema of $w(x,t^n)$, does not exceed the number of extrema of its piecewise-constant projection, $N\left(\sum_j \bar{w}_j^n \chi_j(\cdot)\right)$,

$$N(w(\cdot,t^n)) \leq N\left(\sum_j \bar{w}_j^n \chi_j(\cdot)\right).$$

This non-linear limiter can be modified (see [26]), such that the resulting quadratic reconstruction (1.8), also satisfies a strict maximum principle,

$$\|w(\cdot,t^n)\|_{L^\infty} \leq \left\|\sum_j \bar{w}_j^n \chi_j(\cdot)\right\|_{L^\infty}.$$

Consequently, the corresponding third-order reconstruction is total-variation non-increasing.

Alternatively, one can replace the Taylor prediction (1.13) with a Runge-Kutta solver. For systems, such an approach is more efficient compared with the Taylor expansion, consult [5].

2 Extensions to Two-Dimensions

We start this section with a brief review of the two-dimensional central framework following [14]. This will enable us to introduce the methodology and notations to be used later. We consider the two-dimensional hyperbolic system of conservation laws

$$u_t + f(u)_x + g(u)_y = 0, \tag{2.15}$$

subject to the initial data, $u(x,y,t=0)=u_0(x,y)$. We assume an equally spaced two-dimensional grid; denote by Δx and Δy, the spacing in the x- and in the y-direction, respectively, and denote by $I_{j,k}$ the (j,k)-th cell (see figure 2.2).

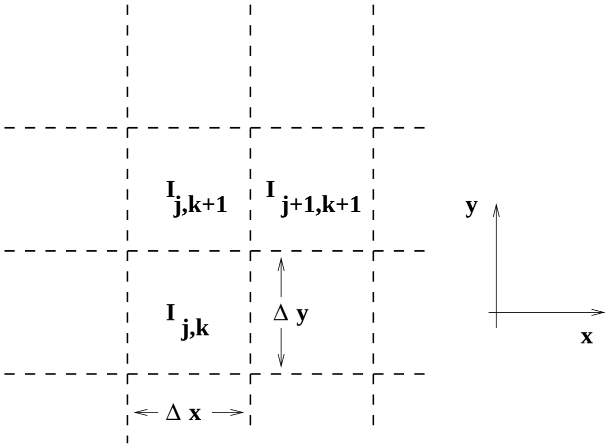

Figure 2.2: Two-dimensional grid

To approximate solutions to (2.15) by a central scheme, we introduce a piecewise-polynomial approximate solution, $w(\cdot,\cdot,t)$, at the discrete time levels, $t^n = n\Delta t$,

$$w(x,y,t^n) = \sum_{j,k} p_{j,k}(x,y)\chi_{j,k}(x,y), \qquad \chi_{j,k}(x,y) := 1_{I_{j,k}}, \tag{2.16}$$

where $p_{j,k}(x,y)$ are polynomials supported at the cells $I_{j,k}$,
$I_{j,k} = I_j \times I_k := \big\{(\xi,\zeta)\,\big|\,|\xi - x_j| \le \frac{\Delta x}{2}, |\zeta - y_k| \le \frac{\Delta y}{2}\big\}$.

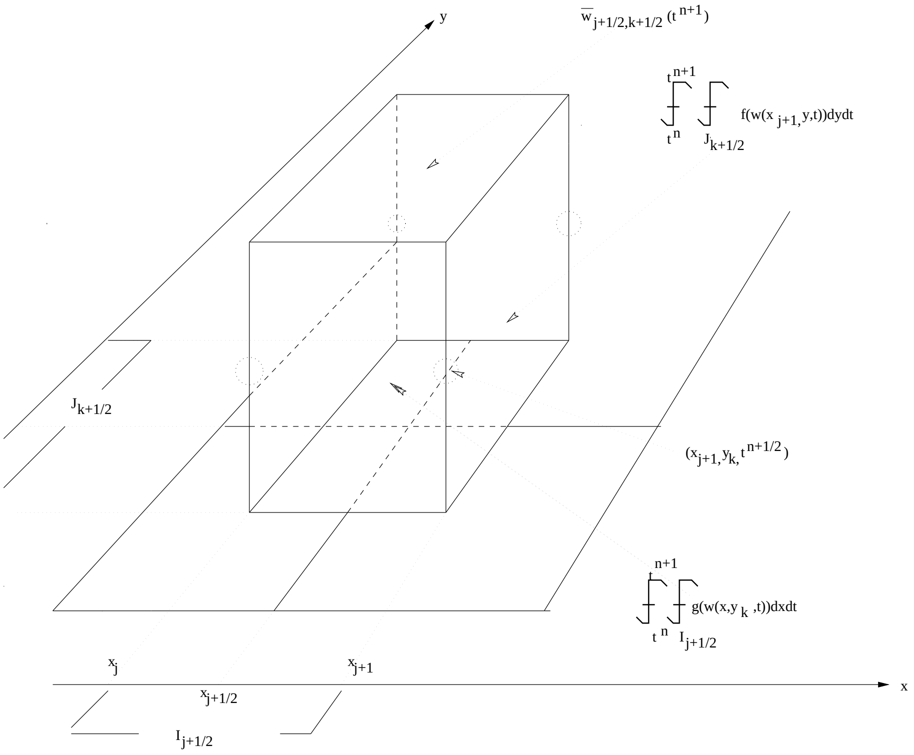

Figure 2.3: The central staggered stencil

An *exact* evolution of w, based on integration of the conservation law (2.15) over the staggered control volume, $I_{j+\frac{1}{2},k+\frac{1}{2}} \times [t^n, t^{n+1}]$, yields (consult figure 2.3)

$$\begin{aligned}
\bar{w}^{n+1}_{j+\frac{1}{2},k+\frac{1}{2}} &= \frac{1}{\Delta x \Delta y}\int\int_{I_{j+\frac{1}{2},k+\frac{1}{2}}} w(x,y,t^n)dydx \qquad (2.17)\\
&- \frac{1}{\Delta x \Delta y}\int_{\tau=t^n}^{t^{n+1}}\left\{\int_{y=y_k}^{y_{k+1}}\left[f\left(w(x_{j+1},y,\tau)\right)-f\left(w(x_j,y,\tau)\right)\right]dy\right\}d\tau\\
&- \frac{1}{\Delta x \Delta y}\int_{\tau=t^n}^{t^{n+1}}\left\{\int_{x=x_j}^{x_{j+1}}\left[g\left(w(x,y_{k+1},\tau)\right)-g\left(w(x,y_k,\tau)\right)\right]dx\right\}d\tau =: \mathcal{I}_1+\mathcal{I}_2.
\end{aligned}$$

Here, $\bar{w}^n_{jk}$, is the cell average at $t = t^n$ associated with the cell I_{jk}, i.e., $\bar{w}_{jk} = \frac{1}{\Delta x \Delta y}\int\int_{I_{jk}} w$. Thus, the first integral on the RHS represents the staggered cell average at time t^n, $\bar{w}^n_{j+\frac{1}{2},k+\frac{1}{2}}$. It consists of contributions from the four neighboring cells,

$$\begin{aligned}
\mathcal{I}_1 = \bar{w}^n_{j+\frac{1}{2},k+\frac{1}{2}} &:= \frac{1}{\Delta x \Delta y}\int\int_{I_{j+\frac{1}{2},k+\frac{1}{2}}} w(x,y,t^n)dydx\\
&= \frac{1}{\Delta x \Delta y}\left[\int_{x_j}^{x_{j+\frac{1}{2}}}\int_{y_k}^{y_{k+\frac{1}{2}}} p_{j,k}(x,y,t^n)dydx + \int_{x_j}^{x_{j+\frac{1}{2}}}\int_{y_{k+\frac{1}{2}}}^{y_{k+1}} p_{j,k+1}(x,y,t^n)dydx\right.\\
&\left.+\int_{x_{j+\frac{1}{2}}}^{x_{j+1}}\int_{y_k}^{y_{k+\frac{1}{2}}} p_{j+1,k}(x,y,t^n)dydx + \int_{x_{j+\frac{1}{2}}}^{x_{j+1}}\int_{y_{k+\frac{1}{2}}}^{y_{k+1}} p_{j+1,k+1}(x,y,t^n)dydx\right].
\end{aligned}$$

These integrals can be evaluated *exactly.* In order to compute the integrals of the fluxes involved in $\mathcal{I}_2$, it remains to recover the point-values $\{w(\cdot,\cdot,\tau)|\ t^n \le \tau \le t^{n+1}\}$, a task which is accomplished in two steps. First, we use the given cell averages to reconstruct the point-values of $w(\cdot,\cdot,t^n)$, reconstructed as a piecewise-polynomial approximation. Second, we follow the evolution of these point-values along the interfaces (x_j, y_k, τ), $t^n \le \tau \le t^{n+1}$. It is here that we take advantage of the finite speed of propagation: thanks to staggering, these interfaces remain free of discontinuities, at least for a sufficiently small time step Δt dictated by the CFL constraint. Hence, the numerical fluxes – which remain bounded away from the propagating singularity at $(x_{j+\frac{1}{2},k+\frac{1}{2}})$, can be computed within any degree of desired accuracy by appropriate quadrature rules.

Below, we present three possible constructions of such central schemes – we start with the first-order two-dimensional Lax-Friedrichs (LxF) scheme. We then proceed by overviewing the second-order scheme by Jiang and Tadmor, [14], which utilizes the MUSCL piecewise-linear interpolant [19]; For a two-dimensional third-order scheme in the context of incompressible flows, we refer to [21], and in the context of compressible flows to [23].

2.1 The Two-Dimensional LxF Scheme

The two-dimensional LxF scheme is based on a piecewise-constant interpolant, where $p_{j,k}(x,y) = \bar{w}^n_{j,k}$, and hence, $w(x,y,t^n) = \sum_{j,k}\bar{w}^n_{j,k}\chi_{j,k}(x,y)$ in (2.16).

In its staggered form, the LxF scheme then supplies the cell-averages at time t^{n+1}, $\bar{w}^{n+1}_{j+\frac{1}{2},k+\frac{1}{2}}$, from the given cell-averages at time t^n, $\bar{w}^n_{j,k}$,

$$\begin{aligned}
\bar{w}^{n+1}_{j+\frac{1}{2},k+\frac{1}{2}} &= \frac{1}{4}(\bar{w}^n_{j,k} + \bar{w}^n_{j+1,k} + \bar{w}^n_{j,k+1} + \bar{w}^n_{j+1,k+1}) \\
&\quad -\frac{\lambda}{2}\left[f(w^n_{j+1,k}) - f(w^n_{j,k}) + f(w^n_{j+1,k+1}) - f(w^n_{j,k+1})\right] \\
&\quad -\frac{\mu}{2}\left[g(w^n_{j,k+1}) - g(w^n_{j,k}) + g(w^n_{j+1,k+1}) - g(w^n_{j+1,k})\right].
\end{aligned} \tag{2.18}$$

Here and below, $\lambda := \frac{\Delta t}{\Delta x}$ and $\mu := \frac{\Delta t}{\Delta y}$, denote the fixed mesh-ratios in the x- and in the y-direction, respectively. The first term on the RHS of (2.18) is the staggered cell-average at time t^n, $\bar{w}^n_{j+1/2,k+1/2}$ and the other two terms there are approximations of the integrals over the fluxes.

2.2 A Two-Dimensional Second-Order Extension

Following the two-dimensional scheme in [14] (see also [2]), which extends the one-dimensional NT scheme in [29], we start with a reconstructed piecewise-linear MUSCL approximation, $w(x,y,t^n) = \sum_{j,k} p_{j,k}(x,y)\chi_{j,k}(x,y)$, where,

$$p_{j,k}(x,y) = \bar{w}^n_{j,k} + w'_{j,k}\left(\frac{x-x_j}{\Delta x}\right) + w^{\backprime}_{j,k}\left(\frac{y-y_k}{\Delta y}\right). \tag{2.19}$$

Here, $w'_{j,k}$ and $w^{\backprime}_{j,k}$, are respectively, the discrete slopes in the x- and in the y-direction, which are reconstructed from the given cell averages. Second-order accuracy is guaranteed wherever these slopes approximate the corresponding derivatives,

$$\left\{\begin{array}{l}
w'_{j,k} \sim \Delta x \cdot w_x(x_j, y_k, t^n) + O(\Delta x)^2, \\[2ex]
w^{\backprime}_{j,k} \sim \Delta y \cdot w_y(x_j, y_k, t^n) + O(\Delta y)^2.
\end{array}\right.$$

In order to prevent oscillations, it is essential to reconstruct these discrete slopes, w' and $w^{\backprime}$, with built-in *limiters*, $1 \le \theta < 2$, e.g. (compare (1.4))

$$\left\{\begin{array}{l}
w'_{j,k} = MM\left\{\theta(\bar{w}^n_{j+1,k} - \bar{w}^n_{j,k}), \frac{1}{2}(\bar{w}^n_{j+1,k} - \bar{w}^n_{j-1,k}), \theta(\bar{w}^n_{j,k} - \bar{w}^n_{j-1,k})\right\} \\[2ex]
w^{\backprime}_{j,k} = MM\left\{\theta(\bar{w}^n_{j,k+1} - \bar{w}^n_{j,k}), \frac{1}{2}(\bar{w}^n_{j,k+1} - \bar{w}^n_{j,k-1}), \theta(\bar{w}^n_{j,k} - \bar{w}^n_{j,k-1})\right\}.
\end{array}\right. \tag{2.20}$$

With this choice of linear approximation, the first term on the RHS of (2.17) – the staggered average, $\bar{w}^n_{j+\frac{1}{2},k+\frac{1}{2}}$, yields by a straightforward computation,

$$\begin{aligned}
\bar{w}^n_{j+\frac{1}{2},k+\frac{1}{2}} &= \frac{1}{4}(\bar{w}^n_{j,k} + \bar{w}^n_{j,k+1} + \bar{w}^n_{j+1,k} + \bar{w}^n_{j+1,k+1}) \\
&\quad +\frac{1}{16}(w'_{j,k} - w'_{j+1,k} + w'_{j,k+1} - w'_{j+1,k+1}) \\
&\quad +\frac{1}{16}(w^{\backprime}_{j,k} - w^{\backprime}_{j,k+1} + w^{\backprime}_{j+1,k} - w^{\backprime}_{j+1,k+1}).
\end{aligned}$$

Next, we turn to the numerical fluxes on the RHS of equation (2.17). They are approximated by the second-order midpoint quadrature rule for the time integral, and by the second-order rectangular quadrature rule for the spatial integration. For example, approximation of the first flux on the right yields

$$\int_{\tau=t^n}^{t^{n+1}} \int_{y=y_k}^{y_{k+1}} f(w(x_{j+1}, y, \tau))dyd\tau \sim \frac{\Delta t \Delta y}{2}(f_{j+1,k}^{n+\frac{1}{2}} + f_{j+1,k+1}^{n+\frac{1}{2}}). \tag{2.21}$$

Analogous expressions hold for the remaining fluxes. The missing mid-values, $w_{j,k}^{n+\frac{1}{2}}$, are predicted using a first-order Taylor expansion (where $\lambda := \frac{\Delta t}{\Delta x}$ and $\mu := \frac{\Delta t}{\Delta y}$ are the usual fixed mesh-ratios),

$$w_{j,k}^{n+\frac{1}{2}} = w_{j,k}^n - \frac{\lambda}{2} f'_{j,k} - \frac{\mu}{2} g^{\backprime}_{j,k}. \tag{2.22}$$

Equipped with these mid-values we are now able to use the approximate fluxes outlined in (2.21), which yield a second-order corrector step of the form

$$\begin{aligned} \bar{w}_{j+\frac{1}{2},k+\frac{1}{2}}^{n+1} &= < \frac{1}{4}(\bar{w}_{j,\cdot}^n + \bar{w}_{j+1,\cdot}^n) + \frac{1}{8}(w'_{j,\cdot} - w'_{j+1,\cdot}) - \lambda(f_{j+1,\cdot}^{n+\frac{1}{2}} - f_{j,\cdot}^{n+\frac{1}{2}}) >_{k+\frac{1}{2}} \\ &+ < \frac{1}{4}(\bar{w}_{\cdot,k}^n + \bar{w}_{\cdot,k+1}^n) + \frac{1}{8}(w^{\backprime}_{\cdot,k} - w^{\backprime}_{\cdot,k+1}) - \mu(g_{\cdot,k+1}^{n+\frac{1}{2}} - g_{\cdot,k}^{n+\frac{1}{2}}) >_{j+\frac{1}{2}} . \end{aligned} \tag{2.23}$$

Here, we employ the following abbreviation for staggered-averaging

$$< w_{j,\cdot} >_{k+\frac{1}{2}} := \frac{1}{2}(w_{j,k} + w_{j,k+1}), \quad < w_{\cdot,k} >_{j+\frac{1}{2}} := \frac{1}{2}(w_{j,k} + w_{j+1,k}).$$

Note that the predictor-corrector central scheme (2.22)-(2.23) is an extension to the canonical first-order Lax-Friedrichs scheme (2.18), based on piecewise-constant reconstruction (with $p_{j,k} \equiv \bar{w}_{j,k}$ and $w'_{j,k} = w^{\backprime}_{j,k} = 0$). It is remarkable that such a relatively simple extension yields a considerable improvement in the resolution of the first-order Lax-Friedrichs scheme while retaining its robust stability properties.

It is well-known that the exact entropy solution of the *scalar* conservation law (2.15) satisfies a maximum principle. Under appropriate CFL condition, the two-dimensional second-order central scheme (2.22) - (2.23) satisfies the same maximum principle. Such maximum principle was originally formulated in [14] in terms of the following

Theorem 2.1 *Consider the two-dimensional scalar scheme (2.22)-(2.23). Assume that the discrete slopes,* w' *and* $w^{\backprime}$*, are reconstructed with the Min-Mod limiter (2.20), and likewise for* $f(w)'$ *and* $g(w)^{\backprime}$*. Then for any* $\theta < 2$*, there exists a sufficiently small CFL number* C_θ*, such that if the CFL condition is fulfilled,*

$$\max(\lambda \cdot \max_u |f_u(u)|, \mu \cdot \max_u |g_u(u)|) \leq C_\theta,$$

then the following local maximum principle holds

$$\min_{\substack{|p-(j+\frac{1}{2})|=\frac{1}{2} \\ |q-(k+\frac{1}{2})|=\frac{1}{2}}} \{\bar{w}_{p,q}^n\} \leq \bar{w}_{j+\frac{1}{2},k+\frac{1}{2}}^{n+1} \leq \max_{\substack{|p-(j+\frac{1}{2})|=\frac{1}{2} \\ |q-(k+\frac{1}{2})|=\frac{1}{2}}} \{\bar{w}_{p,q}^n\}. \tag{2.24}$$

The details of the proof of theorem 2.1 can be found in [14]. The key observation is that the new value, $\bar{w}^{n+1}_{j+\frac{1}{2},k+\frac{1}{2}}$, can be written as a *convex combination* of the cell-averages at t^n, $\bar{w}^n_{j,k}, \bar{w}^n_{j+1,k}, \bar{w}^n_{j,k+1}, \bar{w}^n_{j+1,k+1}$. The proof also utilizes the non-oscillatory properties of the scheme (2.22)-(2.23); reconstructing the slopes with nonlinear limiters (2.20) implies that neighboring discrete slopes cannot have opposite signs. It is therefore possible to bound differences in the slopes in terms of differences of the cell-averages, e.g.

$$|f(w)'_{j+1,k} - f(w)'_{j,k}| \leq \theta |f(\bar{w}^n_{j+1,k}) - f(\bar{w}^n_{j,k})| \leq \theta \max_u |f_u(u)| |\bar{w}^n_{j+1,k} - \bar{w}^n_{j,k}|. \qquad (2.25)$$

Similar expressions hold for the other differences and the proof follows.

References

[1] Anile A. M., Romano V., Russo G., *Extended Hydrodynamical Model of Carrier Transport in Semiconductors*, Phys. Rev. B., to appear.

[2] Arminjon P., Stanescu D., Viallon M.-C., *A Two-Dimensional Finite Volume Extension of the Lax-Friedrichs and Nessyahu-Tadmor Schemes for Compressible Flow*, preprint.

[3] Arminjon P., Viallon M.-C., *Généralisation du Schéma de Nessyahu-Tadmor pour Une Équation Hyperbolique à Deux Dimensions D'espace*, C.R. Acad. Sci. Paris, **t. 320** , série I. (1995), pp. 85-88.

[4] Bereux F., Sainsaulieu L., *A Higher Order Method for the Solution of Hyperbolic Systems with Relaxation*, preprint.

[5] Bianco F., Puppo G., Russo G., *High Order Central Schemes for Hyperbolic Systems of Conservation Laws*, SIAM J. Sci. Comp., to appear.

[6] Engquist B., Runborg O., *Multi-phase Computations in Geometrical Optics*, J. Comp. Appl. Math., in press.

[7] Friedrichs K. O., Lax P. D., *Systems of Conservation Equations with a Convex Extension*, Proc. Nat. Acad. Sci., **68**, (1971), pp.1686-1688.

[8] Godlewski E., Raviart P.-A., *Numerical Approximation of Hyperbolic Systems of Conservation Laws*, Springer, New York, 1996.

[9] Harten A., *High Resolution Schemes for Hyperbolic Conservation Laws*, JCP, **49**, (1983), pp.357-393.

[10] Harten A., Osher S. J., *Uniformly High Order Accurate Non-Oscillatory Scheme. I*, SINUM, **24**, (1982), pp. 229-309.

[11] Huynh H. T., *A Piecewise-parabolic Dual-mesh Method for the Euler Equations*, AIAA-95-1739-CP, The 12th AIAA CFD Conf., 1995.

[12] Jiang G.-S., Levy D., Lin C.-T., Osher S. J., Tadmor E., *High-Resolution Non-Oscillatory Central Schemes with Non-Staggered Grids for Hyperbolic Conservation Laws*, SINUM, to appear.

[13] Jiang G.-S., Shu C.-W., *Efficient Implementation of Weighted ENO Schemes*, JCP, **126**, (1996), pp. 202-228.

[14] Jiang G.-S., Tadmor E., *Nonoscillatory Central Schemes for Multidimensional Hyperbolic Conservation Laws*, SIAM J. Sci. Comp., to appear.

[15] Jin S., private communication.

[16] Kupferman R., *Simulation of Viscoelastic Fluids: Couette-Taylor Flow*, JCP, to appear.

[17] Kupferman R., *A Numerical Study of the Axisymmetric Couette-Taylor Problem Using a Fast High-Resolution Second-Order Central Scheme*, SIAM J. Sci. Comp., to appear.

[18] Kupferman R., Tadmor E., *A Fast High-Resolution Second-Order Central Scheme for Incompressible Flows*, Proc. Nat. Acad. Sci., **94**, (1997), pp. 4848-4852.

[19] van Leer B., *Towards the Ultimate Conservative Difference Scheme, V. A Second-Order Sequel to Godunov's Method*, JCP, **32**, (1979), pp.101-136.

[20] LeVeque R. J., *Numerical Methods for Conservation Laws*, Lectures in Mathematics, Birkhauser Verlag, Basel, 1992.

[21] Levy D., *A Third-order 2D Central Schemes for Conservation Laws*, here.

[22] Levy D., Puppo G., Russo G. *Central Weno Schemes for Hyperbolic Systems of Conservation Lays*, in preparation.

[23] Levy D., Puppo G., Russo G. *Central Weno Schemes for Multi-Dimensional Hyperbolic Systems of Conservation Laws*, in preparation.

[24] Levy D., Tadmor E., *Non-oscillatory Boundary Treatment for Staggered Central Schemes*, submitted.

[25] Levy D., Tadmor E., *Non-oscillatory Central Schemes for the Incompressible 2-D Euler Equations*, Math. Res. Let., **4** (1997), pp.1-20.

[26] Liu X.-D., Osher S., *Nonoscillatory High Order Accurate Self-Similar Maximum Principle Satisfying Shock Capturing Schemes I*, SINUM, **33**, no. 2 (1996), pp.760-779.

[27] Liu X.-D., Osher S., Chan T., *Weighted Essentially Non-oscillatory Schemes*, JCP, **115**, (1994), pp.200-212.

[28] Liu X.-D., Tadmor E., *Third Order Nonoscillatory Central Scheme for Hyperbolic Conservation Laws*, Numer. Math., to appear.

[29] Nessyahu H., Tadmor E., *Non-oscillatory Central Differencing for Hyperbolic Conservation Laws*, JCP, **87**, no. 2 (1990), pp.408-463.

[30] Roe P. L., *Approximate Riemann Solvers, Parameter Vectors, and Difference Schemes*, JCP, **43**, (1981), pp.357-372.

[31] Romano V., Russo G., *Numerical Solution for Hydrodynamical Model of Semiconductors*, IEEE, to appear.

[32] Runborg O., *Multiphase Computations in Geometrical Optics*, UCLA CAM report no. 96-52 (1996).

[33] Sanders R., *A Third-order Accurate Variation Nonexpansive Difference Scheme for Single Conservation Laws*, Math. Comp., **41**, (1988), pp.535-558.

[34] Sanders R., Weiser A., *A High Resolution Staggered Mesh Approach for Nonlinear Hyperbolic Systems of Conservation Laws*, JCP, **1010**, (1992), pp.314-329.

[35] Sod G., *A Survey of Several Finite Difference Methods for Systems of Nonlinear Hyperbolic Conservation Laws*, JCP, **22**, (1978), pp. 1-31.

[36] Sweby P. K., *High Resolution Schemes Using Flux Limiters for Hyperbolic Conservation Laws*, SINUM, **21**, no. 5 (1984), pp.995-1011.

[37] Tadmor E., *Approximate Solutions of Nonlinear Conservation Laws*, CIME Lecture notes, 1997, UCLA CAM Report 97-51.

[38] Tadmor E., Wu C.C., *Central Scheme for the Multidimensional MHD Equations*, in preparation.